

# BoundPlanner: A convex-set-based approach to bounded manipulator trajectory planning

Thies Oelerich<sup>1</sup>, Christian Hartl-Nesic<sup>1</sup>, Florian Beck<sup>1</sup>, Andreas Kugi<sup>1,2‡</sup>

Preprint

## Abstract

Online trajectory planning enables robot manipulators to react quickly to changing environments or tasks. Many robot trajectory planners exist for known environments but are often too slow for online computations. Current methods in online trajectory planning do not find suitable trajectories in challenging scenarios that respect the limits of the robot and account for collisions. This work proposes a trajectory planning framework consisting of the novel Cartesian path planner based on convex sets, called BoundPlanner, and the online trajectory planner BoundMPC [1]. BoundPlanner explores and maps the collision-free space using convex sets to compute a reference path with bounds. BoundMPC is extended in this work to handle convex sets for path deviations, which allows the robot to optimally follow the path within the bounds while accounting for the robot's kinematics. Collisions of the robot's kinematic chain are considered by a novel convex-set-based collision avoidance formulation independent on the number of obstacles. Simulations and experiments with a 7-DoF manipulator show the performance of the proposed planner compared to state-of-the-art methods. The source code is available at [github.com/Thieso/BoundPlanner](https://github.com/Thieso/BoundPlanner) and videos of the experiments can be found at [www.acin.tuwien.ac.at/42d4](http://www.acin.tuwien.ac.at/42d4).

## 1 INTRODUCTION

Modern robots are equipped with numerous sensors, e.g., cameras and F/T sensors, enabling them to act autonomously in unknown situations and solve tasks requiring flexibility like household tasks [2]. For example, tidying up a room is challenging due to the unstructured environment in which the robot has to act. It is infeasible to provide a complete description of such an environment as it is prone to changes. Obstacles like chairs, tables, and humans may change locations at any time. The robot needs to move fluently and quickly, which presents a major challenge for trajectory planning. Planning robot motions is difficult due to kinematic, dynamic and collision-avoidance constraints making offline planners [3, 4, 5] a common choice. However, it is important to plan robotic motions online and react quickly in order to address the challenges of unstructured and dynamic environments. Popular approaches are online optimization-based trajectory planning with a receding horizon [6, 1, 2, 7] or sampling-based trajectory planning [8, 9].

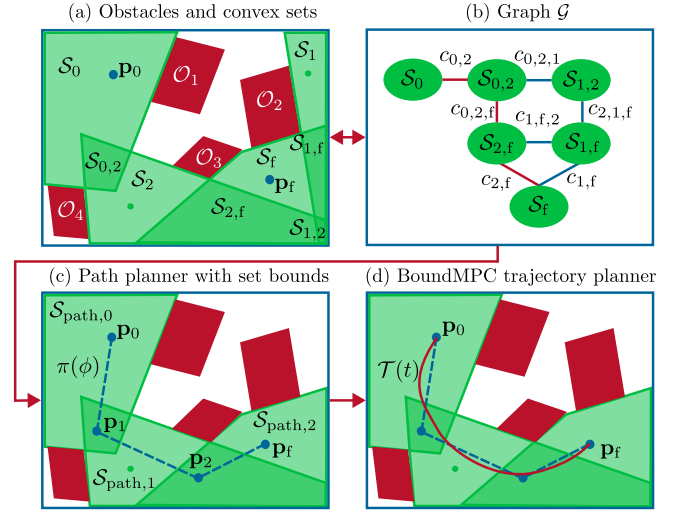


**Figure 1:** Schematic of the path planning using *BoundPlanner* to plan a Cartesian path  $\pi(\phi)$  from the start point  $\mathbf{p}_0$  to the end point  $\mathbf{p}_f$ . (a) The graph  $\mathcal{G}$  is built using the convex sets  $\mathcal{S}_0, \mathcal{S}_1, \mathcal{S}_2, \mathcal{S}_f$  around  $\mathbf{p}_0, \mathbf{p}_f$ , and the green sample points, further visualized in (b). (c) A sequence of convex sets  $\mathcal{S}_{\text{path},0}, \dots, \mathcal{S}_{\text{path},2}$  is found using  $\mathcal{G}$ , connecting the starting set  $\mathcal{S}_0$  with the ending set  $\mathcal{S}_f$ . A path  $\pi(\phi)$  is constructed inside these sets connecting  $\mathbf{p}_0$  with  $\mathbf{p}_f$ . (d) BoundMPC [1] uses the path  $\pi(\phi)$  of *BoundPlanner* to find a suitable joint trajectory  $\mathcal{T}(t)$  such that the end-effector stays within the convex sets, thus avoiding the obstacles  $\mathcal{O}_1, \dots, \mathcal{O}_4$ .

Collision objects divide the environment into a collision-free and an occupied space. Solving a trajectory planning problem to move between two points in these clustered spaces may yield multiple solutions. This makes it challenging to plan motions online. For robot manipulators, potential functions are often used for online planning [9, 6, 8]. Such a formulation generates costs in a cost function when the robot is close to a collision, but it does not guarantee collision avoidance and can lead to issues with, e.g., thin obstacles. Furthermore, the resulting cost terms depend on the number of obstacles that scale poorly to environments with many obstacles, e.g., when using point clouds. Alternatively, convex sets in the joint space are used in [4] to describe the collision-free space. However, it is computationally expensive to compute such sets since obstacles are given in the

<sup>\*\*</sup>This work was not supported by any organization.

<sup>†1</sup>All authors are with the Automation and Control Institute (ACIN), TU Wien, Vienna, Austria, {oelerich, hartl, beck, kugi}@acin.tuwien.ac.at

<sup>‡2</sup>Andreas Kugi is with the center for Vision, Automation & Control, AIT Austrian Institute of Technology GmbH, Vienna, Austria [andreas.kugi@ait.ac.at](mailto:andreas.kugi@ait.ac.at)

task space and are not trivially transferred to the joint space. This prohibits online planning. The work in [10] proposes a method to learn differentiable bounds along a path, but these bounds are not guaranteed to be collision-free. In the Cartesian position space, convex sets are simple to compute and are used for trajectory planning in [2, 11, 12]. This approach scales well even for environments given as point clouds [11].

The trajectory planning problem may be separated into two subproblems by first computing a reference path as a geometrical curve in space and then finding a trajectory that follows this reference path [1, 13]. The reference path, computed by, e.g., [5, 14, 2], provides global guidance for the subsequent path-following controller [15, 16, 17, 1]. If the reference path considers the robot's kinematics and collisions, the path may be followed exactly, but such a path is difficult to compute. Therefore, the works [18, 1, 19] propose to allow path deviations. This idea is also used in [1] and [2] to follow Cartesian paths under consideration of the robot's kinematics. Bounds around the path ensure collision freedom while allowing the trajectory planner to deviate from the path to account for kinematic constraints. The work in [1, 2] shows that this is advantageous when executing the robot's motion compared to following a Cartesian path exactly.

This work proposes a trajectory planner for robot manipulators, consisting of a novel convex-set-based Cartesian path planner called *BoundPlanner* and the MPC-based trajectory planner *BoundMPC*. The former performs fast reference path planning in Cartesian space and allows reactive online re-planning using convex collision-free sets. The latter computes the robot trajectory online to follow the reference path while allowing deviations from the path within the convex sets to consider the robot's kinematics. The main contributions of this work are

- a fast Cartesian path planner, which explores the collision-free space by computing convex sets,
- an extension to *BoundMPC* [20] to exploit convex sets as path deviation bounds,
- a novel collision avoidance formulation for the entire robot manipulator, making trajectory planning independent of the number of obstacles.

## 2 BoundPlanner

The proposed method, called *BoundPlanner* is explained in detail in this section. The objective of *BoundPlanner* is to compute a bounded path  $\pi(\phi)$  given the initial pose of the robot's end-effector with position  $\mathbf{p}_0$  and rotation matrix  $\mathbf{R}_0$  and the desired final pose defined by  $\mathbf{p}_f$  and  $\mathbf{R}_f$ . A schematic overview of the method is shown in Fig. 1. A graph  $\mathcal{G}$  of collision-free convex sets is used to plan the Cartesian reference path  $\pi(\phi)$  for the robot's end-effector with convex sets  $\mathcal{S}_{\text{path},i}$  as Cartesian bounds. This path is then used by the model predictive control (MPC) framework *BoundMP* [20] in Section 3 to compute the trajectory  $\mathcal{T}(t)$  online by following the created reference path within the given bounds to reach the goal. The bounds ensure that the motion is restricted to the collision-free convex sets of the created graph.

## 2.1 Collision-free Convex Sets

This section describes the procedure of finding collision-free convex sets in the Cartesian position space in a bounded domain  $\mathcal{D} \subset \mathbb{R}^3$  with  $K$  convex obstacles  $\mathcal{O}_k$ ,  $k = 1, \dots, K$ . In this work, a convex position set  $\mathcal{S}$  is defined by a set of  $S$  half spaces parametrized by a matrix  $\mathbf{A} \in \mathbb{R}^{S \times 3}$  and a vector  $\mathbf{b} \in \mathbb{R}^S$ , i.e.,  $\mathcal{S} = \{\mathbf{x} \in \mathcal{D} : \mathbf{A}\mathbf{x} \leq \mathbf{b}\}$ . The following subsections describe three ways to obtain such convex sets, i.e., two methods based on ellipsoid volume maximization, and one method using a given set of points.

### 2.1.1 Ellipsoid Volume Maximization

A convex set  $\mathcal{S}$  defines a unique ellipsoid  $\mathcal{E}$ , specified by its shape matrix  $\mathbf{C}_{\mathcal{E}}$  and midpoint  $\mathbf{p}_{\mathcal{E}}$ , inscribed into  $\mathcal{S}$  with maximum volume, i.e.,  $\mathcal{E}$  is the maximum-volume inscribed ellipsoid (MVIE). Computing  $\mathcal{E}$  in  $\mathcal{S}$  is a convex optimization problem that can be solved efficiently. The works [21] and [11] use an iterative procedure to find large collision-free convex sets using MVIE as follows. First, an initial collision-free ellipsoid is specified around a given seed point in the collision-free space. Second, an initial convex set is computed for this ellipsoid using MVIE. Third, an iterative procedure is employed in which the ellipsoid  $\mathcal{E}$  and the convex set  $\mathcal{S}$  are computed alternately. For more information, the reader is referred to [21] and [11]. The algorithm in [11] uses a second-order cone optimization which is considerably faster than the semidefinite programming approach [21]; hence [11] is used in this work. Two different variants of finding  $\mathcal{S}$  are considered, namely

- *MVIE* optimizes all values of the ellipsoid  $\mathcal{E}$ , i.e.,  $\mathbf{C}_{\mathcal{E}}$  and  $\mathbf{p}_{\mathcal{E}}$ ,
- *MVIE-fixed-mid* optimizes only  $\mathbf{C}_{\mathcal{E}}$  of the ellipsoid  $\mathcal{E}$ , while  $\mathbf{p}_{\mathcal{E}}$  remains fixed.

The *MVIE-fixed-mid* problem may be thought of as finding the largest convex set  $\mathcal{S}$  around the point  $\mathbf{p}_{\mathcal{E}}$ , whereas the *MVIE* problem does not need to contain  $\mathbf{p}_{\mathcal{E}}$ .

### 2.1.2 Convex Hull Set

The problems *MVIE* and *MVIE-fixed-mid* cannot guarantee that a certain set of points is contained in the convex set  $\mathcal{S}$ . Therefore, a third way is introduced, i.e., finding a convex set around a set  $\mathcal{S}_{\text{ch}}$  defined as the convex hull of the points  $\mathbf{p}_{\text{ch},j}$ ,  $j = 1, \dots, J$ . In order to compute the set  $\mathcal{S}$ , the points on an obstacle  $\mathcal{O}_k$ ,  $k = 1, \dots, K$ , and the set  $\mathcal{S}_{\text{ch}}$  with the smallest distance are determined using

$$\arg \min_{\mathbf{p}_{\text{ch}}^* \in \mathcal{S}_{\text{ch}}, \mathbf{p}_{\mathcal{O}_k}^* \in \mathcal{O}_k} \|\mathbf{p}_{\mathcal{O}_k}^* - \mathbf{p}_{\text{ch}}^*\|_2^2 \quad (1)$$

The vector  $\mathbf{a}_k = \mathbf{p}_{\mathcal{O}_k}^* - \mathbf{p}_{\text{ch}}^*$  defines a half space to separate the obstacle  $\mathcal{O}_k$  from the set  $\mathcal{S}_{\text{ch}}$ . The corresponding half space distance is computed as  $b_k = \mathbf{a}_k^T \mathbf{p}_{\mathcal{O}_k}^*$  such that the half space touches the obstacle  $\mathcal{O}_k$ . Together,  $\mathbf{a}_k$  and  $b_k$  constitute  $\mathbf{A}$  and  $\mathbf{b}$  and thus define  $\mathcal{S}$ . To improve the computational efficiency, the half spaces are computed starting with the closest obstacle. Obstacles further away are disregarded if the half space also separates the set  $\mathcal{S}_{\text{ch}}$  from such obstacles. Generally, this procedure is computationally more

efficient than the ellipsoid-based computations but does not optimize for the set volume. This defines the third way of computing a collision-free set  $\mathcal{S}$  in this work:

- *Set-convex-hull* compute  $\mathcal{S}$  around the convex set  $\mathcal{S}_{\text{ch}}$ .

## 2.2 Graph of Collision-free Convex Sets

In this section, the graph  $\mathcal{G}$  of convex sets and a path  $\pi_{\mathcal{G}}$  through this graph are computed. The end-effector geometry is modeled as a convex hull defined by the set of points  $\mathbf{p}_{e,l}(\phi)$ ,  $l = 1, \dots, L$ . Hence, the path  $\pi_{\mathcal{G}}$  connects the start set  $\mathcal{S}_0$ , containing of the entire convex hull of the end-effector at its initial position  $\mathbf{p}_0$  with its initial orientation  $\mathbf{R}_0$ , with the final set  $\mathcal{S}_f$ , containing the entire end-effector at its final position  $\mathbf{p}_f$  and orientation  $\mathbf{R}_f$ . To this end, the convex sets  $\mathcal{S}_0$  and  $\mathcal{S}_f$  are computed using *Set-convex-hull* around the known end-effector hull in the known orientations  $\mathbf{R}_0$  and  $\mathbf{R}_f$  at  $\mathbf{p}_0$  and  $\mathbf{p}_f$ , respectively.

To find the structure of the collision-free space, multiple convex sets are computed in the domain  $\mathcal{D}$  and a graph  $\mathcal{G}$  is built based on set intersections. Two convex sets  $\mathcal{S}_a$  and  $\mathcal{S}_b$  intersect if their intersection set  $\mathcal{S}_{a,b}$  is not empty, i.e.,  $\mathcal{S}_{a,b} = \mathcal{S}_a \cap \mathcal{S}_b \neq \emptyset$ . In this work, the graph  $\mathcal{G}$  describes the collision-free space with the intersection sets as its vertices and connecting sets as edges. An edge between two vertices indicates that the intersection sets (vertices) have a common set (edge) as part of the intersection. The edge cost  $c_{a,b,c}$  between the two intersection sets  $\mathcal{S}_{a,b}$  and  $\mathcal{S}_{b,c}$

$$c_{a,b,c} = c_{\text{size},b} \|\mathbf{p}_{a,b} - \mathbf{p}_{b,c}\|_2 + c_{\text{bias}} \quad (2)$$

is proportional to the distance between the two intersection sets  $\mathcal{S}_{a,b}$  and  $\mathcal{S}_{b,c}$ , approximated by the points  $\mathbf{p}_{a,b} \in \mathcal{S}_{a,b}$  and  $\mathbf{p}_{b,c} \in \mathcal{S}_{b,c}$ , plus a bias cost  $c_{\text{bias}} > 0$  to penalize set transitions. The size cost  $c_{\text{size},b}$  is chosen as

$$c_{\text{size},b} = 1 + w_{\text{size}} \tanh\left(\frac{1}{2} - \sqrt[3]{\det(\mathbf{C}_{\mathcal{E},b})}\right), \quad (3)$$

with  $0 < w_{\text{size}} \leq 1$  and the determinant of the MVIE in  $\mathcal{S}_b$  as an approximation of the volume of  $\mathcal{S}_b$ . Next assume that a new set  $\mathcal{S}_a$  is added to the graph intersecting with  $\mathcal{S}_b$ . Then the intersection set  $\mathcal{S}_{a,b}$  is assigned the point

$$\mathbf{p}_{a,b} = \min_{\mathbf{p} \in \mathcal{S}_{a,b}} \|\mathbf{p} - \mathbf{p}_b\|_2^2, \quad (4)$$

which is the projection of  $\mathbf{p}_b$  onto the intersection set  $\mathcal{S}_{a,b}$ . Each intersection set  $\mathcal{S}_{a,b}$  is assigned a point  $\mathbf{p}_{a,b}$  to compute the edge cost (2). The point  $\mathbf{p}_b$  is equal to  $\mathbf{p}_0$  or  $\mathbf{p}_f$  for the start and end sets, respectively, which is then iteratively projected when a new set is added to graph  $\mathcal{G}$ . If neither the start set  $\mathcal{S}_0$  nor the end set  $\mathcal{S}_f$  are intersected and no prior projections are available, the two closest points in the intersection sets are used. The graph-building process is visualized in Fig. 2 for the example scenario in Fig. 1. Note that an intersection set is added to graph  $\mathcal{G}$  in Fig. 1 only if the end-effector fits inside the intersection set using the end-effector description introduced below in Section 2.4.

## 2.3 Exploring the Environment with Collision-free Convex Sets

Optimally, each point in the collision-free subspace  $\mathcal{D}_{\text{free}} \subset \mathcal{D}$  of the entire planning domain  $\mathcal{D}$  is contained in at least

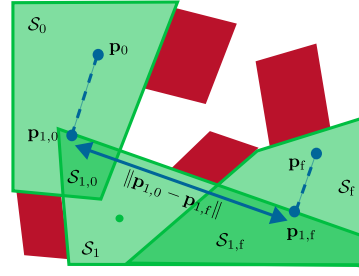


**Figure 2:** Graph building procedure of BoundPlanner. The set  $\mathcal{S}_1$  intersects with the starting set  $\mathcal{S}_0$  and the final set  $\mathcal{S}_f$ . In order to compute the costs  $c_{0,1,f}$  from (2) for the edge between the intersection sets  $\mathcal{S}_{1,0}$  and  $\mathcal{S}_{1,f}$ , the projections  $\mathbf{p}_{1,0}$  and  $\mathbf{p}_{1,f}$  are computed using (4).

one convex set in graph  $\mathcal{G}$ . In order to explore  $\mathcal{D}_{\text{free}}$ , the collision-free space is sampled and convex sets are computed around each sample point, which are further referred to as seed points. This sampling is performed until a path  $\pi_{\mathcal{G}}$  connecting  $\mathcal{S}_0$  and  $\mathcal{S}_f$  is found in graph  $\mathcal{G}$ . In this work, rejection sampling is used, and the intersections of the computed convex sets are added to graph  $\mathcal{G}$  using the procedure of the previous section. The rejection sampling rejects seed points within an obstacle  $\mathcal{O}_k$  or within a previously computed convex set. The sample will thus be in the unexplored space of  $\mathcal{D}_{\text{free}}$ .

**Remark.** *This sampling approach is probabilistically complete, i.e., the collision-free subspace  $\mathcal{D}_{\text{free}} \subset \mathcal{D}$  will be covered by convex sets as the number of samples grows to infinity. Each seed point is contained in its respective convex set. Thus, if a solution exists, it will eventually be found.*

The path  $\pi_{\mathcal{G}}$  is the shortest path of sets through the graph  $\mathcal{G}$  using Dijkstra's algorithm [22]. Once a valid path  $\pi_{\mathcal{G}}$  is found, a refinement step is performed. For this, new convex sets are computed with the projection points  $\mathbf{p}_{a,b}$  as seed points and are added to  $\mathcal{G}$ . Successively, a new path  $\pi_{\mathcal{G}}$  is computed through this graph. This procedure is iteratively repeated until the path converges. The optimal path  $\pi_{\mathcal{G}}$  through the graph is finally obtained as a series of edges defined by the sets  $\mathcal{S}_{\text{path},i}$ ,  $i = 0, \dots, N$ , where  $\mathcal{S}_{\text{path},0} = \mathcal{S}_0$  and  $\mathcal{S}_{\text{path},N} = \mathcal{S}_f$ .

An overview of the algorithm of BoundPlanner is given as pseudocode in Algorithm 1. Adding a new set  $\mathcal{S}_a$  to the graph  $\mathcal{G}$ , including the computation of the intersections and costs, is represented by the function `add_set_to_graph( $\mathcal{G}, \mathcal{S}_a$ )`. It returns the connected flag, indicating if a connection between the start and the end set exists in graph  $\mathcal{G}$ . The path refinement step is indicated by the `refining` flag. The last two lines are explained in the next section

## 2.4 Path Planning within the Graph of Convex Sets

This section explains the procedure of finding a reference path  $\pi$  from the path of sets  $\pi_{\mathcal{G}}$  from Section 2.2. The reference path  $\pi(\phi)$  consists of a position reference path  $\pi_p(\phi)$  and an orientation reference path  $\pi_o(\phi)$  in rotation matrix form. Both are assumed piecewise linear where a linear ori-

---

**Algorithm 1** BoundPlanner

---

**Require:** Starting pose  $\mathbf{p}_0, \mathbf{R}_0$  and final pose  $\mathbf{p}_f, \mathbf{R}_f$ , domain  $\mathcal{D}$ , obstacles  $\mathcal{O}_k$   
 $\mathcal{S}_0 \leftarrow \text{Set-convex-hull around } \mathbf{p}_0, \mathbf{R}_0 \quad \triangleright \text{Set around start}$   
 $\mathcal{S}_f \leftarrow \text{Set-convex-hull around } \mathbf{p}_f, \mathbf{R}_f \quad \triangleright \text{Set around end}$   
 $\mathcal{G} \leftarrow \{\}$   $\triangleright \text{Initialize graph of convex sets}$   
 $\text{add\_set\_to\_graph}(\mathcal{G}, \mathcal{S}_0)$   
 $\text{connected} \leftarrow \text{add\_set\_to\_graph}(\mathcal{G}, \mathcal{S}_f)$   
 $\text{success} \leftarrow \text{False}$   
 $\text{refining} \leftarrow \text{False}$   
 $\pi_{\mathcal{G}, \text{old}} \leftarrow \emptyset$   
 $i = 1$   
**while**  $\text{success} = \text{False}$  **do**  
  **if**  $\text{connected} = \text{True}$  **then**  
     $\pi_{\mathcal{G}} \leftarrow \text{dijkstras\_algorithm}(\mathcal{G})$   
    **if**  $\pi_{\mathcal{G}} = \pi_{\mathcal{G}, \text{old}}$  **then**  
       $\text{success} \leftarrow \text{True}$   
       $\mathbf{p}_{\text{samples}} \leftarrow \{\}$   
    **else**  
       $\text{refining} \leftarrow \text{True}$   
       $\mathbf{p}_{\text{samples}} \leftarrow \{\mathbf{p}_{a,b} \mid \forall (a,b) : \mathcal{S}_{a,b} \in \pi_{\mathcal{G}}\}$   
       $\pi_{\mathcal{G}, \text{old}} = \pi_{\mathcal{G}}$   
    **end if**  
  **else**  
     $\text{refining} \leftarrow \text{False}$   
     $\mathbf{p}_{\text{samples}} \leftarrow \text{sample } \mathbf{p} \in \mathcal{D}_{\text{free}}$   
  **end if**  
  **for**  $\mathbf{p} \in \mathbf{p}_{\text{samples}}$  **do**  
    **if**  $\text{refining} = \text{True}$  **then**  
       $\mathcal{S}_i \leftarrow \text{MVIE-fixed-mid around } \mathbf{p}$   
    **else**  
       $\mathcal{S}_i \leftarrow \text{MVIE around } \mathbf{p}$   
    **end if**  
     $\text{connected} \leftarrow \text{add\_set\_to\_graph}(\mathcal{G}, \mathcal{S}_i)$   
     $i = i + 1$   
  **end for**  
**end while**  
 $\pi_p, \pi_o \leftarrow \text{solve (8)}$   $\triangleright \text{Reference paths}$   
**return**  $\pi_p, \pi_o, \pi_{\mathcal{G}}$

---

entation path is given by a constant spatial angular velocity as in [1]. The path parameter  $\phi$  determines the progress along the path. As mentioned, the set of points  $\mathbf{p}_{e,l}(\phi)$ ,  $l = 1, \dots, L$  define the convex hull of the end-effector geometry. Point  $\mathbf{p}_e(\phi)$  is the end-effector position for which the position and orientation paths are planned. The points  $\mathbf{p}_{e,l}(\phi)$  are expressed relative to  $\mathbf{p}_e(\phi)$  as

$$\mathbf{p}_{e,l}(\mathbf{p}_e(\phi), \mathbf{R}_e(\phi)) = \mathbf{p}_e(\phi) + \mathbf{R}_e(\phi) \mathbf{l}_{e,l}, l = 1, \dots, L, \quad (5)$$

with the constant offset vectors of the hull points  $\mathbf{l}_{e,l}$ .

The poses that define the piecewise linear paths  $\pi_p(\phi)$  and  $\pi_o(\phi)$  are called via-points. Each intersection set between two consecutive sets  $\mathcal{S}_{\cap,i} = \mathcal{S}_{\text{path},i} \cap \mathcal{S}_{\text{path},i+1}$ ,  $i = 0, \dots, N-1$ , in  $\pi_{\mathcal{G}}$  contains one via-point. Hence, the piece-

wise linear position path

$$\pi_p(\phi) = \begin{cases} \mathbf{p}_0 + (\phi - \phi_0) \mathbf{v}_0 & \phi_0 \leq \phi < \phi_1 \\ \vdots & \vdots \\ \mathbf{p}_{N-1} + (\phi - \phi_{N-1}) \mathbf{v}_{N-1} & \phi_{N-1} \leq \phi < \phi_N \\ \mathbf{p}_N = \mathbf{p}_f & \phi = \phi_N, \end{cases} \quad (6)$$

with the positions  $\mathbf{p}_i \in \mathcal{S}_{\cap,i}$  and unit-norm direction vectors  $\mathbf{v}_i = (\mathbf{p}_{i+1} - \mathbf{p}_i) / \|\mathbf{p}_{i+1} - \mathbf{p}_i\|_2$ , has exactly one linear path segment in each convex set  $\mathcal{S}_{\text{path},i}$ . Setting  $\phi_{i+1} - \phi_i = \|\mathbf{p}_{i+1} - \mathbf{p}_i\|_2$  ensures continuity of the path (6). Due to the convexity property, each segment from  $\mathbf{p}_i$  to  $\mathbf{p}_{i+1}$  is entirely contained in  $\mathcal{S}_{\text{path},i+1}$ , and, thus, the whole piecewise linear position path is contained in  $\pi_{\mathcal{G}}$ . Note that this containment is only valid for the end-effector position  $\mathbf{p}_e(\phi)$  but disregards the extent of the end-effector. In order to account for the end-effector's extent, the points  $\mathbf{p}_{e,l}(\pi_p(\phi), \pi_o(\phi))$  are enforced to be within the corresponding set. The paths for these points depend on the orientation of the end-effector. The orientation path  $\pi_o(\phi)$  starts at  $\pi_o(0) = \mathbf{R}_0$  and ends at  $\pi_o(\phi_f) = \mathbf{R}_f$ . As a simplification, the orientation path is assumed to be a piecewise linear path with a piecewise constant spatial angular velocity composed of a constant unit-norm direction  $\omega_{\text{ref}}$  and the magnitudes  $\alpha_i$ , i.e.,

$$\pi_o(\phi) = \begin{cases} \text{Exp}(\alpha_0 \frac{\phi - \phi_0}{\phi_1 - \phi_0} \omega_{\text{ref}}) \mathbf{R}_0 & \phi_0 \leq \phi < \phi_1 \\ \vdots & \vdots \\ \text{Exp}(\alpha_{N-1} \frac{\phi - \phi_{N-1}}{\phi_N - \phi_{N-1}} \omega_{\text{ref}}) \mathbf{R}_{N-1} & \phi_{N-1} \leq \phi < \phi_N \\ \mathbf{R}_N = \mathbf{R}_f & \phi = \phi_N. \end{cases} \quad (7)$$

**Remark.** The simplification in (7) is introduced to simplify the path-finding problem. This is a performant choice which is applicable to many motions in practice. Future work will explore ways to improve this simplification.

The direction  $\omega_{\text{ref}}$  is given by the shortest connection, i.e., the geodesic between the initial and final orientation. The intermediate orientations are iteratively defined as  $\mathbf{R}_i = \text{Exp}(\alpha_{i-1} \omega_{\text{ref}}) \mathbf{R}_{i-1}$ ,  $i = 1, \dots, N$ . Hence, the path  $\pi$  is constructed using (6) and (7) from the via-points  $\mathbf{p}_i$  and the magnitudes  $\alpha_i$  only. The optimization problem

$$\begin{aligned} & \min_{\mathbf{p}_i, \alpha_i} \sum_{i=1}^{N-2} c_{\text{size,path},i} (\|\mathbf{p}_{i+1} - \mathbf{p}_i\|_2^2 + w_\alpha \|\alpha_{i+1} - \alpha_i\|_2^2) \\ & \text{s.t. } \mathbf{p}_i \in \mathcal{S}_{\cap,i}, i = 1, \dots, N-1 \\ & \quad \mathbf{p}_{e,l}(\pi_p(\phi), \pi_o(\phi)) \in \mathcal{S}_{\text{path},i} \\ & \quad \phi_{i-1} < \phi < \phi_i, l = 1, \dots, L, i = 1, \dots, N \\ & \quad \mathbf{p}_{e,l}(\pi_p(\phi_i), \pi_o(\phi_i)) \in \mathcal{S}_{\cap,i} \\ & \quad l = 1, \dots, L, i = 1, \dots, N-1, \end{aligned} \quad (8)$$

with  $w_\alpha > 0$ , finds these parameters to obtain the shortest reference path  $\pi(\phi)$  through  $\pi_{\mathcal{G}}$  such that the end-effector and all hull points remain inside the convex sets  $\mathcal{S}_{\text{path},i}$ . The size cost  $c_{\text{size,path},i}$  is computed using (3), which favors large sets over small sets. The first constraint in (8) ensures that the position path  $\pi_p(\phi)$  is contained in the convex sets  $\mathcal{S}_{\cap,i}$ .

The other constraints ensure that the convex hull of the end-effector is contained in the convex sets for all values of  $\phi$ , which needs additional considerations. With the convex set  $\mathcal{S}_{\text{path},i}$  for  $\phi_i < \phi < \phi_{i+1}$ ,  $i = 0, \dots, N-1$ , the hull points  $\mathbf{p}_{e,l}(\pi_p(\phi), \pi_o(\phi))$  have distances

$$\mathbf{d}_{\text{path},i}(\phi) = \mathbf{A}_{\text{path},i} \mathbf{p}_{e,l}(\pi_p(\phi), \pi_o(\phi)) - \mathbf{b}_{\text{path},i} \quad (9)$$

to the half spaces of  $\mathcal{S}_{\text{path},i}$  defined by  $\mathbf{A}_{\text{path},i}$  and  $\mathbf{b}_{\text{path},i}$ . As the orientation path  $\pi_o(\phi)$  follows the geodesic between the initial orientation  $\mathbf{R}_0$  and desired orientation  $\mathbf{R}_f$ , the maximum angle traversed by the orientation path is  $180^\circ$ . Geometrically each hull point moves along a circle in Cartesian space combined with a linear motion due to the linear position path  $\pi_p$  in (6). Hence, the function (9) is either a convex or a concave function for each element  $d_{\text{path},i,s}$ ,  $s = 1, \dots, S$ , of  $\mathbf{d}_{\text{path},i}$ . The minima  $\phi_{\min}^T = [\phi_{\min,1}, \dots, \phi_{\min,N}]$  of (9) are at

$$\phi_{\min,i} = \arg \min_{\phi_{i-1} < \phi < \phi_i} d_{\text{path},i,s}(\phi), s = 1, \dots, S, \quad (10)$$

which simplifies the second constraint in (8) to

$$\mathbf{A}_{\text{path},i} \mathbf{p}_{e,l}(\pi_p(\phi_{\min,i}), \pi_o(\phi_{\min,i})) \leq \mathbf{b}_{\text{path},i} \quad (11)$$

$$l = 1, \dots, L, i = 1, \dots, N.$$

This results in a finite number of constraints, making (8) solvable. Since the gradients of (6) are discontinuous, at the via-points Euler spirals [23] are used to smooth the path  $\pi_p(\phi)$ .

### 3 BoundMPC with Convex Sets as Bounds

The BoundMPC [1] framework computes optimal joint-space trajectories in constrained Cartesian spaces along reference paths  $\pi_p(\phi)$  and  $\pi_o(\phi)$  using a discrete planning horizon of  $M$  time steps. The reader is referred to [1] for a full description of the framework. This section describes the adaption of BoundMPC to handle the path  $\pi(\phi)$  with the convex sets  $\mathcal{S}_{\text{path},i}$  as path bounds which BoundPlanner computes in Section 2.

#### 3.1 Convex Sets as Path Bounds

Having obtained the reference path  $\pi(\phi)$  with (6)–(8), the bounds for the position path  $\pi_p(\phi)$  are determined in the following. The original work [1] uses polynomials along basis vectors to limit the deviations from the path, which were fitted to collision-free convex sets in [2]. However, this yields conservative approximations since the end-effector is bound to be within a basis-vector-aligned rectangle at each path point. In contrast, this work uses the constraint

$$\mathbf{g}_{\text{set}} = \mathbf{A}_{\text{path},i} \mathbf{p}_{\text{tcp}}(t) \leq \mathbf{b}_{\text{path},i} \quad (12)$$

$$\phi_{i-1} < \phi(t) < \phi_i, i = 1, \dots, N$$

for bounding deviations in BoundMPC, where  $\mathbf{p}_{\text{tcp}}(t)$  is the position of the end-effector at time  $t$ . Note that the position  $\mathbf{p}_{\text{tcp}}(t)$  is not necessarily on the path and thus differs from  $\mathbf{p}_e(\phi)$ .

The planned reference path  $\pi(\phi)$  ensures a collision-free robot motion only for the end-effector along the reference position path  $\pi_p(\phi)$  with the reference orientation path  $\pi_o(\phi)$ . In order to consider the entire robot kinematics for general robot manipulators, this work uses a novel formulation for collision avoidance based on convex sets. This is presented here for  $R$  arbitrary points on the robot  $\mathbf{p}_{c,r}(t)$ ,  $r = 1, \dots, R$ , that need to be collision checked at all times  $t$ . The collision constraint for the trajectory planning at time  $t$  becomes simply

$$\mathbf{A}_{c,r} \mathbf{p}_{c,r} \leq \mathbf{b}_{c,r}, r = 1, \dots, R, \quad (13)$$

with individual convex sets  $\mathcal{S}_{c,r}$  defining the half spaces  $\mathbf{A}_{c,r}$  and  $\mathbf{b}_{c,r}$ . The sets  $\mathcal{S}_{c,r}$  are found by solving the *Set-convex-hull* problem. The points  $\mathbf{p}_{\text{ch},j}$  defining the convex hull are set to the position  $\mathbf{p}_{\text{ch},1} = \mathbf{p}_{c,r}(t)$  at the current time  $t$  and the estimated position  $\mathbf{p}_{\text{ch},2} = \hat{\mathbf{p}}_{c,r}(t_h)$  at time  $t_h$  at the end of the planning horizon of the previous MPC iteration, respectively. Note that the convex hull of two points is a line which makes (1) analytically solvable. Consequently, the formulation (13) defines the collision-free space for each point  $\mathbf{p}_{c,r}$  instead of defining the obstacle-occluded space as is commonly done in robotics [6, 1, 24]. Convex sets are easy to formulate mathematically and to compute.

The constraint formulation (13) has the advantage of being independent of the number of obstacles  $\mathcal{O}_k$  as it only requires the convex sets  $\mathcal{S}_{c,r}$ . While this approach is generally more conservative than describing the obstacle-occluded space, it yields good solutions in practice. The computation of the sets depends on the number of obstacles and is generally fast, even for a large number of obstacles [11]. This becomes especially relevant when working with point clouds since they consist of hundreds or thousands of points.

**Remark.** The points  $\mathbf{p}_{c,r}$  may be used to describe the robot collision model using spheres. As it is commonly done, the size of the obstacles is extended by the radius of the sphere corresponding to the robot dimensions at  $\mathbf{p}_{c,r}$ .

#### 3.2 Horizon splitting

The path bounds in the original paper [1] are described by polynomials along basis directions. In contrast, this work uses the constraint (12). However, directly enforcing (12) is undesirable since the constraint is not continuous. Instead, the switching points between two consecutive path sets are determined before the optimization such that the BoundMPC optimization remains continuous. This is implemented based on the idea of horizon splitting [6]. Imagine that the current horizon of the end-effector position trajectory  $\mathbf{p}_{\text{horizon},m}$ ,  $m = 1, \dots, M$ , spans two path sets  $\mathcal{S}_{\text{path},i}$  and  $\mathcal{S}_{\text{path},i+1}$ . The splitting index

$$m_s = \min_m (\phi > \phi_i - \epsilon_\phi) \quad (14)$$

$$\wedge \mathbf{p}_{\text{horizon},m} \in \mathcal{S}_{\text{path},i}$$

$$\wedge \mathbf{p}_{\text{horizon},m} \in \mathcal{S}_{\text{path},i+1}$$

with tolerance  $\epsilon_\phi \geq 0$  is determined by the set membership of the end-effector position at each time step in the horizon.



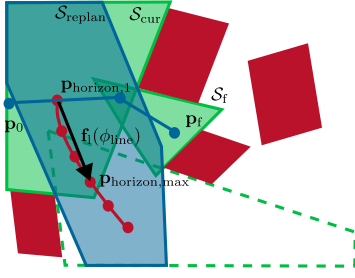


**Figure 3:** Schematic drawing of the replanning procedure where the replanning happens in  $S_{\text{cur}}$ . The replanning set  $S_{\text{replan}}$  is computed to include  $\mathbf{p}_{\text{horizon},1}$  and  $\mathbf{p}_{\text{horizon},\text{max}}$ .

This leads to the constraint

$$\mathbf{g}_{\text{split}} = \begin{cases} \mathbf{A}_{\text{path},i} \mathbf{p}_{\text{horizon},m} \leq \mathbf{b}_{\text{path},i}, & m < m_s \\ \mathbf{A}_{\text{path},i+1} \mathbf{p}_{\text{horizon},m} \leq \mathbf{b}_{\text{path},i+1}, & m \geq m_s. \end{cases} \quad (15)$$

Furthermore, a terminal constraint is added based on the first set that is outside the horizon  $S_{\text{path},i+2}$  which guides the robot along the path. Particularly, the terminal constraint limits the path deviations such that the robot can transition into  $S_{\text{path},i+2}$ , guiding it along the path. Lastly, constraint (13) is added to account for collisions of the robot's kinematic chain.

### 3.3 Replanning

The fast computation of the reference paths  $\pi_p(\phi)$  and  $\pi_o(\phi)$  combined with the replanning capabilities of BoundMPC [1] enables online replanning of the reference paths. This procedure is illustrated in Fig. 3. To ensure feasibility after the replanning event, it is important to account for the current robot state. The current planning horizon computed by BoundMPC includes  $M$  discretized end-effector positions  $\mathbf{p}_{\text{horizon},m}$ ,  $m = 1, \dots, M$ . The current end-effector position  $\mathbf{p}_{\text{horizon},1}$  is contained in the current set  $S_{\text{cur}}$  defined by  $\mathbf{A}_{\text{cur}}$  and  $\mathbf{b}_{\text{cur}}$ . Then, the point

$$\begin{aligned} \mathbf{p}_{\text{horizon},\text{max}} &= \max_m \mathbf{p}_{\text{horizon},m} \\ \text{s.t. } &\mathbf{A}_{\text{cur}} \mathbf{p}_{\text{horizon},m} \leq \mathbf{b}_{\text{cur}} \end{aligned} \quad (16)$$

is the temporally farthest-away point in the planning horizon that is still within the current set  $S_{\text{cur}}$ .

The starting point during the replanning procedure is set to  $\mathbf{p}_0 = \mathbf{p}_{\text{horizon},1}$ , for which a starting set  $S_{\text{replan}}$  is computed using the *Set-convex-hull* approach with  $\mathbf{p}_{l,0} = \mathbf{p}_{\text{horizon},1}$  and  $\mathbf{p}_{l,1} = \mathbf{p}_{\text{horizon},\text{max}}$  such that the first and last point in the horizon are inside the set  $S_{\text{replan}}$ . This set is then used as  $S_0$  in Algorithm 1. After replanning, the path  $\pi_p(\phi)$  should be extended at  $\mathbf{p}_0$  to ensure proper projection onto the new reference path with BoundMPC. This is indicated visually in Fig. 3.

## 4 Experiments

The proposed planning method is evaluated in two scenarios. The first scenario in Section 4.1 requires the 7-DoF KUKA LBR iiwa 14 R820 robot to turn around and reach into a box. In the second scenario in Section 4.2, the manipulator must

grasp an object from a shelf but the object changes its position during the approaching motion such that online replanning is required.

### 4.1 Scenario 1: Reach into box

This scenario is depicted in Fig. 4. The robot must reach into a box where an additional obstacle above the box significantly complicates the trajectory planning. The robot has to move from an open space into a very restricted space in the box. The depicted path sets  $S_{\text{path},i}$ ,  $i = 0, 1, 2$ , cover a large portion of the free space  $\mathcal{D}_{\text{free}}$ . Using BoundPlanner and BoundMPC, the robot's end-effector trajectory  $\mathbf{p}_{\text{tcp}}(t)$  successfully traverses the convex sets to the final position  $\mathbf{p}_f$  with the final orientation  $\mathbf{R}_f$ . Large deviations of the trajectory  $\mathbf{p}_{\text{tcp}}(t)$  from the reference path  $\pi_p(\phi)$  are observed to account for the kinematic constraints of the robot. Collision avoidance is considered for the end-effector by constraining the end-effector position  $\mathbf{p}_{\text{tcp}}(t)$  to the path sets  $S_{\text{path},i}$  and for the rest of the kinematic chain using the constraint (13) with  $R = 5$  points  $\mathbf{p}_{c,r}$  along the chain. The points  $\mathbf{p}_{c,r}$  are chosen on the joint axes 3, 4, and 6 and between joint 6 and the end-effector. The evolution of the collision-free set  $S_{c,5}$  for the point  $\mathbf{p}_{c,5}$  over time is depicted in Fig. 5. The margins around the obstacles account for the size of the robot around  $\mathbf{p}_{c,5}$ . The convex sets capture the space around the point and allow the robot to move into the strongly constrained space around the final pose, showing the effectiveness of the proposed collision avoidance constraint (13) and the iterative update of  $S_{c,5}$ . Note that due to their convex nature, the sets  $S_{c,5}$  are a conservative approximation of the free space around  $\mathbf{p}_{c,5}$ , but this does not degrade performance in practice.

BoundPlanner with BoundMPC is also compared to state-of-the-art approaches, namely the graph-of-convex-sets (GCS) approach from [4], VP-STO [9], and a bidirectional RRT [3] approach with a tracking MPC that minimizes the tracking error with respect to the reference trajectory. The GCS method requires the final joint configuration as a goal for trajectory planning and seed points in joint space to explore the collision-free space. Both inputs are generally hard to provide and are not required by BoundPlanner. Hence, for the comparison, the seed points are provided manually as in [4] and consist of six configurations, including the start and end configuration. VP-STO [9] is a global planner that directly plans joint trajectories based on a Cartesian description of the obstacles. Collision-freeness of the trajectory is enforced in the cost function. The final joint configuration is provided to VP-STO since it does not converge otherwise. However, no intermediate joint configurations, as in GCS, are needed for the planner. The RRT approach uses a bidirectional RRT [3] to plan a reference path in position space. The corresponding orientations are computed as interpolations between the start and end orientation. The reference trajectory, consisting of position and orientation, is obtained as a spline [25]. A trajectory-tracking MPC is then used to track the reference trajectory to minimize the tracking error. Collisions are avoided using potential functions [6].

The computed trajectories for all methods are visually compared in Fig. 4. BoundPlanner with BoundMPC and VP-STO create short Cartesian trajectories and reach the final

**Table 1:** Open-box scenario: Comparison of BoundPlanner with GCS, RRT+MPC and VP-STO for eight different box placements. The reported values are the mean values of the end-effector trajectory length for position  $l_{\text{traj},p}$  and orientation  $l_{\text{traj},o}$ , the planning time  $t_{\text{plan}}$ , and the trajectory duration  $T_{\text{traj}}$ .

	BoundPlanner	GCS	RRT + MPC	VP-STO
$l_{\text{traj},p} / \text{m}$	1.07	3.56	0.89	1.45
$l_{\text{traj},o} / ^\circ$	140	659	130	188
$t_{\text{plan}} / \text{s}$	0.11	233.15	0.51	9.3
$T_{\text{traj}} / \text{s}$	5.3	13.67	5.4	4.21
Failures	0	1	4	0

point  $\mathbf{p}_f$ . The GCS method also converges to the final point but has a considerably longer trajectory in Cartesian space. Finally, the RRT+MPC method gets stuck in a local minimum before the box and cannot reach the final pose. In order to further evaluate the robustness of the methods, eight different placements of the open box are considered and evaluated in Table 1 for all methods. The lengths  $l_{\text{traj},p}$  and  $l_{\text{traj},o}$  for the Cartesian end-effector trajectory indicate short trajectories for the proposed BoundPlanner method due to the Cartesian planning. The planning time  $t_{\text{plan}}$  is the lowest for our proposed method making it possible to start and replan the movement online. Furthermore, no failures occur using BoundPlanner, whereas RRT+MPC often gets stuck in local minima due to the simple tracking objective. BoundPlanner only specifies a planning volume instead of minimizing the tracking error, allowing more freedom during the robot's motion. Hence, BoundPlanner can reliably compute collision-free paths and tracking volumes for the entire kinematic chain in constrained environments. The GCS planner fails once despite providing the desired end configuration and the six seed configurations because the convex sets do not allow for a connection between the start and end configuration. Also, GCS generally has longer Cartesian trajectories with long planning times  $t_{\text{plan}}$ . VP-STO successfully solves the task and has lower trajectory durations  $T_{\text{traj}}$  than the MPC-based planners but requires significantly longer planning times  $t_{\text{plan}}$ , which are not suitable for online replanning.

## 4.2 Scenario 2: Grasp from shelf with replanning

In the second scenario, visualized in Fig. 6, the robot grasps an object in different locations that change during the approach motion and require replanning. In this scenario, BoundPlanner with BoundMPC and RRT+MPC are considered, as GCS and VP-STO exhibit too long planning times  $t_{\text{plan}}$ . The end-effector trajectories in Fig. 6 for both methods contain two exemplary replanning events. At the start, the robot plans toward  $\mathbf{p}_{f,1}$ , and shortly before arriving, the final point is changed to  $\mathbf{p}_{f,2}$  that is repeated for the final replanning toward  $\mathbf{p}_{f,3}$ . Both methods perform the replanning quickly and reach the final point  $\mathbf{p}_{f,3}$ . However, the RRT+MPC method plans a trajectory that collides with the shelf after the second replanning. This collision is attributed to the robot prioritizing the minimization of the tracking error over the collision avoidance. This is avoided by BoundMPC as the convex sets used for collision avoidance do not allow

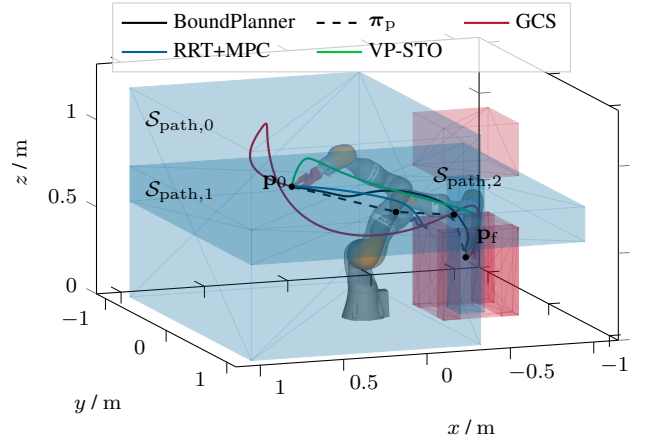


**Figure 4:** Open-box scenario: The robot has to turn around and reach in the box with its end-effector. The convex obstacles  $\mathcal{O}_k$ ,  $k = 1, \dots, 5$ , are depicted in red and the convex planning sets  $\mathcal{S}_{\text{path},i}$ ,  $i = 0, \dots, 2$ , in blue. The end-effector trajectories  $\mathbf{p}_{\text{tcp}}(t)$  of different methods as well as the reference path  $\pi_p(\phi)$  of BoundPlanner are shown.

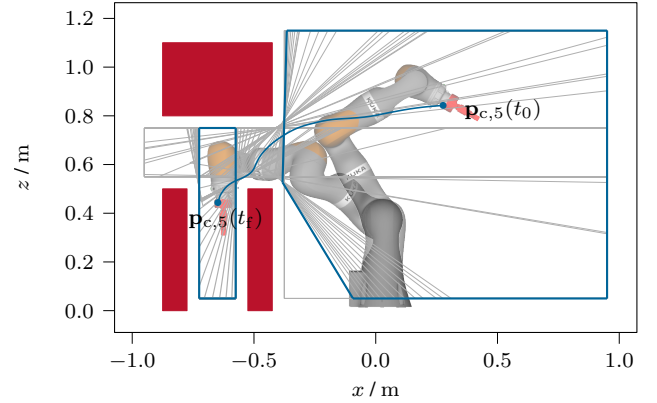


**Figure 5:** Open-box scenario: Collision avoidance sets for the point  $\mathbf{p}_{c,5}$  on the robot's kinematic chain. The set  $\mathcal{S}_{c,5}$  for the initial time  $t_0$  and the final time  $t_f$  is shown in blue and at intermediate time steps in grey. The grey lines illustrate the evolution of  $\mathcal{S}_{c,5}$  over time with increasing line width.

for such trade-offs resulting in safe and collision-free trajectories for the robot.

The robustness of random replanning events is further evaluated for 20 replannings, performed for random positions. The replannings happen shortly before reaching the desired pose. The results in Table 2 show that the replanning times  $t_{\text{plan}}$  of BoundPlanner are generally faster, and the trajectories are collision-free. The collisions of MPC+RRT are attributed to the same phenomenon as in Fig. 6.

## 5 Conclusions

A novel Cartesian path planner based on convex sets, called BoundPlanner, is proposed in this work for fast planning in cluttered environments for robot manipulators. Furthermore, the online trajectory planner BoundMPC was extended to handle convex sets as bounds, allowing a robot to safely execute complex manipulation tasks in confined spaces using

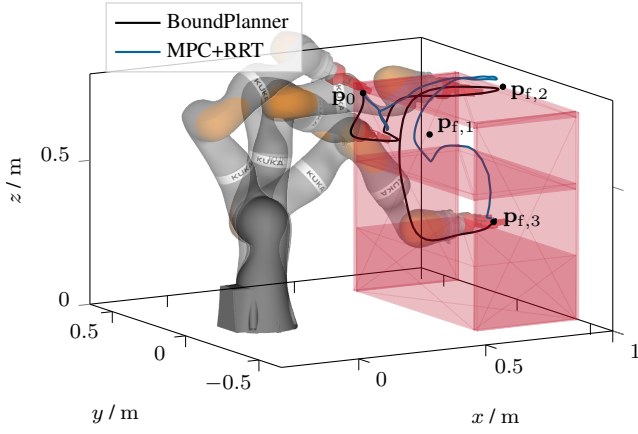


**Figure 6:** Replanning scenario: The robot has to grasp an object from a shelf, but the object changes its position from  $\mathbf{p}_{f,1}$  to  $\mathbf{p}_{f,2}$  and finally to  $\mathbf{p}_{f,3}$  during the robot's motion. The convex obstacles  $O_k, k = 1, \dots, 5$ , are depicted in red. The end-effector trajectories  $\mathbf{p}_{tcp}(t)$  of BoundPlanner and MPC+RRT are shown.

**Table 2:** Replanning scenario: Comparison of BoundPlanner with RRT+MPC for 20 random replanning events.

	BoundPlanner			RRT+MPC		
	min	avg	max	min	avg	max
$t_{\text{plan}} / \text{s}$	0.04	0.1	0.17	0.02	0.54	2.06
Number of collisions	0			3		

a novel collision avoidance formulation for the entire robot kinematics based on convex sets. The proposed approach was compared with state-of-the-art methods on a 7-DoF robot manipulator in two scenarios. The first scenario requires the robot to grasp into a box in a strongly constrained environment where the novel collision avoidance is demonstrated and the fast planning times compared to global planners are highlighted. In the second scenario, the replanning capabilities of BoundPlanner are demonstrated to create safe and performant trajectories online. In future work, BoundPlanner will be embedded in a higher-level task-planning and decision-making framework to solve long-horizon manipulation tasks safely and reliably.

## References

- [1] Thies Oelerich, Florian Beck, Christian Hartl-Nesic, and Andreas Kugi. BoundMPC: Cartesian Path Following with Error Bounds based on Model Predictive Control in the Joint Space. *The International Journal of Robotics Research (in press)*, 2024, DOI 10.1177/02783649241309354.
- [2] Thies Oelerich, Christian Hartl-Nesic, and Andreas Kugi. Language-guided Manipulator Motion Planning with Bounded Task Space. In *Proceedings of the Conference on Robot Learning (CoRL) (in press)*, 2024.
- [3] Steven M. LaValle. *Planning Algorithms*. Cambridge University Press, first edition, 2006.
- [4] Tobia Marcucci, Mark Petersen, David von Wrangel, and Russ Tedrake. Motion planning around obstacles with convex optimization. *Science Robotics*, 8(84):eadf7843, 2023.
- [5] Mohamed Elbanhawi and Milan Simic. Sampling-Based Robot Motion Planning: A Review. *IEEE Access*, 2:56–77, 2014.
- [6] Florian Beck, Minh Nhat Vu, Christian Hartl-Nesic, and Andreas Kugi. Model Predictive Trajectory Optimization With Dynamically Changing Waypoints for Serial Manipulators. *IEEE Robotics and Automation Letters*, 9(7):6488–6495, 2024.
- [7] Tobias Schoels, Per Rutquist, Luigi Palmieri, Andrea Zanelli, Kai O. Arras, and Moritz Diehl. CIAO\*: MPC-based safe motion planning in predictable dynamic environments. *IFAC-PapersOnLine*, 53(2):6555–6562, 2020.
- [8] Mohak Bhardwaj, Balakumar Sundaralingam, Arsalan Mousavian, Nathan Ratliff, Dieter Fox, Fabio Ramos, and Byron Boots. STORM: An Integrated Framework for Fast Joint-Space Model-Predictive Control for Reactive Manipulation. In *Proceedings of the Conference on Robot Learning (CoRL)*, volume 164, pages 750–759, 2022.
- [9] Julius Jankowski, Lara Bruder Müller, Nick Hawes, and Sylvain Calinon. VP-STO: Via-point-based Stochastic Trajectory Optimization for Reactive Robot Behavior. In *Proceedings of the IEEE International Conference on Robotics and Automation (ICRA)*, pages 10125–10131, 2023.
- [10] Jon Arrizabalaga, Zachary Manchester, and Markus Ryll. Differentiable Collision-Free Parametric Corridors. In *arXiv: 2407.12283*, 2024.
- [11] Qianhao Wang, Zhepei Wang, Mingyang Wang, Jialin Ji, Zhichao Han, Tianyue Wu, Rui Jin, Yuman Gao, Chao Xu, and Fei Gao. Fast Iterative Region Inflation for Computing Large 2-D/3-D Convex Regions of Obstacle-Free Space. In *arXiv: 2403.02977v2*, 2024.
- [12] Yulin Li, Chunxin Zheng, Kai Chen, Yusen Xie, Xindong Tang, Michael Yu Wang, and Jun Ma. Collision-Free Trajectory Optimization in Cluttered Environments Using Sums-of-Squares Programming. *IEEE Robotics and Automation Letters*, 9(12):11026–11033, 2024.
- [13] Robin Verschueren, Niels van Duijkeren, Jan Swevers, and Moritz Diehl. Time-optimal motion planning for n-DOF robot manipulators using a path-parametric system reformulation. In *Proceedings of the American Control Conference (ACC)*, pages 2092–2097, 2016.
- [14] Sven Mikael Persson and Inna Sharf. Sampling-based A\* algorithm for robot path-planning. *The International Journal of Robotics Research*, 33(13):1683–1708, 2014.



- [15] Timm Faulwasser, Benjamin Kern, and Rolf Findeisen. Model Predictive Path-Following for Constrained Non-linear Systems. In *Proceedings of the IEEE Conference on Decision and Control (CDG)*, pages 8642–8647, 2009.
- [16] Niels Van Duijkeren, Robin Verschueren, Goele Pipeleers, Moritz Diehl, and Jan Swevers. Path-following NMPC for serial-link robot manipulators using a path-parametric system reformulation. In *Proceedings of the European Control Conference (ECC)*, pages 477–482, Aalborg, Denmark, 2016.
- [17] Christian Hartl-Nesic, Tobias Glück, and Andreas Kugi. Surface-based path following control: Application of curved tapes on 3-D objects. *IEEE Transactions on Robotics*, 37(2):615–626, 2021.
- [18] Angel Romero, Sihao Sun, Philipp Foehn, and Davide Scaramuzza. Model Predictive Contouring Control for Time-Optimal Quadrotor Flight. *IEEE Transactions on Robotics*, 38(6):3340–3356, 2022.
- [19] Jon Arrizabalaga and Markus Ryll. Towards Time-Optimal Tunnel-Following for Quadrotors. In *Proceedings of the International Conference on Robotics and Automation (ICRA)*, pages 4044–4050, 2022.
- [20] Thies Oelerich, Christian Hartl-Nesic, and Andreas Kugi. Model Predictive Trajectory Planning for Human-Robot Handovers . In *Proceedings of the VDI Mechatronics Conference*, 2024.
- [21] Robin Deits and Russ Tedrake. Computing Large Convex Regions of Obstacle-Free Space Through Semidefinite Programming. In *Algorithmic Foundations of Robotics XI*, volume 107, pages 109–124. Springer, Cham, 2015.
- [22] E. W. Dijkstra. A note on two problems in connexion with graphs. *Numerische Mathematik*, 1:269–271, 1959.
- [23] Arthur Newell Talbo. *The Railway Transition Spiral*. New York: McGraw-Hill, 1915.
- [24] M. N. Vu, P. Zips, A. Lobe, F. Beck, W. Kemmetmüller, and A. Kugi. Fast motion planning for a laboratory 3D gantry crane in the presence of obstacles. *IFAC-PapersOnLine*, 53(2):9508–9514, 2020.
- [25] Marc Toussaint, Jason Harris, Jung-Su Ha, Danny Driess, and Wolfgang Hönig. Sequence-of-Constraints MPC: Reactive Timing-Optimal Control of Sequential Manipulation. In *Proceedings of the International Conference on Intelligent Robots and Systems (IROS)*, pages 13753–13760, 2022.